



The influence of slopes on interrill erosion processes using loessial soil

Bing Wu^{1,2,3} · Ludi Li¹ · Ling Xu¹ · Xindong Wei⁴ · Xinlu Li¹

Received: 3 March 2021 / Accepted: 1 July 2021 / Published online: 20 July 2021
© The Author(s), under exclusive licence to Springer-Verlag GmbH Germany, part of Springer Nature 2021

Abstract

Purpose The influence of slope gradient on interrill erosion processes is a key scientific problem in the decision-making process regarding soil erosion control in Loess Plateau. The relationship of time to runoff (RT), flow velocity (V), runoff rate (RR) and interrill erosion rate (IER) with slope gradient was investigated to derive accurate experimental model to evaluate and quantify the influence of slopes on interrill erosion processes.

Materials and methods The experimental soil was collected from Ansai County of Shaanxi Province, China. The average diameter of the test soil was 0.041 mm. The experiment was conducted at slopes of 8.74%, 17.62%, 26.78%, 36.38%, 46.6%, 57.70% and 69.97% under I of 90, 120 and 150 mm h⁻¹, respectively, using indoor simulated rainfall. Time to runoff, flow velocity, runoff rate and interrill erosion rate were measured for each combination.

Results and discussion Results showed that the time to runoff decreased as a linear function with increasing slope gradient. Slope gradient was a good predictor of time to runoff for different rainfall intensities with NSE from 0.90 to 0.97 and MSE from 0.1 to 0.25 and R² from 0.90 to 0.97. The flow velocity increased as a power function with increasing slope gradients. Slope gradient was a good predictor of flow velocity for different rainfall intensities with NSE from 0.91 to 0.93 and MSE from 0.01 to 0.015 and R² from 0.95 to 0.98. The runoff rate increased as a power function with increasing slope gradients. Slope gradient was a good predictor of runoff rate for different rainfall intensities with NSE from 0.90 to 0.95 and MSE from 0.000000024 to 0.000000044 and R² from 0.94 to 0.97. The interrill erosion rate increased as a power function with increasing slope gradients. Slope gradient was a good predictor of interrill erosion rate for different rainfall intensities with NSE from 0.98 to 0.99 and MSE from 0.00022 to 0.00055 and R² from 0.98 to 0.99.

Conclusions By performing the controlled simulated rainfall experiments, this study showed that slopes strongly influenced interrill erosion processes for different rainfall intensities.

Keywords Slope gradient · Time to runoff · Flow velocity · Runoff rate · Interrill erosion rate

1 Introduction

The Loess Plateau in China is one of the serious soil erosion regions in the world (Shi and Shao 2000; Zhang et al. 2009; Liu et al. 2012b; Zhao et al. 2013). Interrill erosion processes

are one of the major erosion processes in the Loess Plateau (Liu et al. 2012a), and the slope gradient was one of the major factors that influence interrill erosion processes (Zhang et al. 2019; Zhang 2019). Interrill erosion processes on loess hillslope, which are regarded as an important and indispensable water erosion processes, are accompanied by

Responsible editor: Lu Zhang

✉ Ling Xu
xuling82@xjtu.edu.cn

✉ Xindong Wei
xindongw@chd.edu.cn

¹ Department of Civil Engineering, School of Human Settlements and Civil Engineering, Xi'an Jiaotong University, Xi'an 710049, Shaanxi, China

² State Key Laboratory of Earth Surface Processes and Resource Ecology, Beijing Normal University, Beijing 100000, China

³ State Key Laboratory of Soil Erosion and Dryland Farming On the Loess Plateau, Institute of Water and Soil Conservation, Chinese Academy of Sciences and Ministry of Water Resources, Yangling 712100, Shaanxi, China

⁴ Shaanxi Key Laboratory of Land Consolidation, School of Land Engineering, Chang'an University, Xi'an 710054, Shaanxi, China

a large amount of water resource loss of sheet flow and its aggravation to rill erosion, ephemeral gully erosion and total water erosion on steep slopes. Thus, how to evaluate and quantify the influence of slope gradient on interrill erosion processes is a key scientific problem in the decision-making process regarding soil erosion control in this area.

Many researchers conducted different experiments to study interrill erosion processes based on different experiment conditions. Fox and Bryan (2000) found that the linear or less than linear relationship between interrill erosion rate and slope gradient using sandy loam soil and the slope gradients were from 2.5 to 40%; Ben-Hur and Wakindiki (2004) found that slope gradients have a positive influence on total soil loss using the kaolinitic, clayey smectitic and sandy loam smectitic soils and the slope gradients were from 9 to 25%; Assouline and Ben-Hur (2006) found that cumulative runoff at the end of the rainfall event was lower as slopes were steeper, while an opposite trend was obtained for soil loss using sandy soil and the slope gradients were from 5 to 25%; and Armstrong et al. (2011) studied the interrill erosion using silt loam soils under the slope gradients from 3 to 9% and found that at slope angles representative of agricultural land soil erosion does not increase with slope as traditionally assumed and that the runoff and erosion response is very variable. Shi et al. (2013) found that the relation between interrill erosion rate and mulch rate was best described by an exponential function using silty clay loam; Zhao et al. (2014) evaluated the influence of soil surface roughness on interrill erosion rate under the rainfall intensity of 60 mm/h and the slope gradient of 17.62% and found that the interrill erosion rate decreased as the soil surface roughness increased; Fu et al. (2011) studied the influence of slopes on total splash loss, net downslope splash loss and wash loss and found that the total splash loss, net downslope splash loss and wash loss all increased with slope, and then decreased after a maximum value was reached. Cao et al. (2015) studied the interrill erosion on unpaved roads under the slope gradients of 10.5–26.8% and found that slope gradients are key factors to model surface runoff and sediment yield. Wu et al. (2017a) studied the influence of slope gradients on flow velocity and runoff rate based on model calculations and found that flow velocity and runoff rate increased with increasing slope gradient on mild slopes, and decreased after a critical slope gradient. Zhang and Wang (2017) studied the influence of slope length on interrill erosion rate and found that slope length was negatively related to interrill erosion rate. Wu et al. (2017b) evaluated the relationships between sheet erosion rate and hydrodynamic parameters and found that stream power was the best predictor of sheet erosion. Li et al. (2018) found that slope gradient had only a minor effect on overland flow and sediment yield under the slope gradients of 4.3% and 13.1%. Wang et al. (2018) found that herbaceous vegetation

can reduce and control sheet erosion by reducing the effect of rainfall intensity or slope, especially under sufficiently high vegetation cover. Zhang et al. (2019) studied the effect of tillage on sheet erosion and found that tillage patterns had an obvious effect on sheet erosion.

Although the interrill erosion processes were studied under different slope gradients, different rainfall intensities, different slope lengths, different tillage patterns, different surface roughness, and so on, almost all studies achieved the gentle slope gradient and the studies on steep slope gradients were mainly aimed at the evolution of interrill erosion processes and the relationship between interrill erosion rate and hydrodynamic parameters (i.e. shear stress, stream power and unit stream power). The Loess Plateau in northwest China is characterized by different slopes including gentle slope gradients, steep slope gradients and very steep slope gradients. Govers (1992) determined that no existing formula could perform efficiently over the entire range of available data. Hence, conducting experiments under this condition is necessary to obtain an improved understanding of the interrill erosion process in this region.

The objectives of this study are (1) to evaluate and quantify the influence of slope gradient on interrill erosion processes including time to runoff, flow velocity, runoff rate and interrill erosion rate and (2) to establish new and reliable experimental models between interrill erosion processes and slope gradients. The results can deeply reveal interrill erosion processes and provide a scientific basis for soil erosion control in the area.

2 Methods and materials

2.1 Experiment equipment

2.1.1 Simulated rainfall device

The experiments were conducted in the Simulation Rainfall Hall operated by the State Key Laboratory of Soil Erosion and Dryland Farming on the Loess Plateau in Yangling, Shaanxi Province, China. A rainfall simulator system with three nozzles on two sides was used to produce simulated rainfall. The fall height of raindrops sprayed from the nozzles was approximately 16 m above the soil surface in all the experiments. The raindrop diameters of the simulated rainfall were from 0.125 to 6.0 mm; moreover, the raindrop median volume diameters were from 1.52 to 2.7 mm. In addition, the raindrop kinetic energies of the simulated rainfall were from 201.76 to 1059.95 J m⁻² h⁻¹, and the raindrop terminal velocities were from 1.5 to 8.1 m s⁻¹. The simulated rainfall, with uniformity higher than 90%, exhibited similar raindrop size and distribution to those of natural rainfall. The rainfall simulator system used in the study was same as that used in Shen et al. (2016) and Wu et al. (2017a, b, c, 2018).

2.1.2 Soil pan

Each experiment soil pan with metal frames was 100 cm long, 50 cm wide and 50 cm deep, and the size of the experiment soil pan was similar to that utilized in Vaezi et al. (2017) (140 cm long, 100 cm wide and 15 cm deep) and Ding and Huang (2017) (100 cm long, 20 cm wide and 15 cm deep). The slope gradient for this soil pan could be adjusted between 0 and 80%.

2.2 Experimental soil

The experimental soil was collected from Ansai County (109°19' E, 36°51' N) of Shaanxi Province, China. It consisted of 37.31% sand (diameter 0.05–2.0 mm), 51.30% silt (diameter 0.002–0.05 mm) and 11.39% clay (diameter < 0.002 mm). The average diameter of the test soil was 0.041 mm. The experimental soil, which was highly erodible, was silty loam based on the soil texture classification system of the US Department of Agriculture.

2.3 Experiment setup

The complete combinations of seven slope gradients (8.74%, 17.62%, 26.78%, 36.38%, 46.6%, 57.70% and 69.97%) and three rainfall intensities (90, 120 and 150 mm h⁻¹) were included in the experiment with 2 replicates. Before packing the soil to the experiment soil pan, its water content and the bulk density were adjusted to 14% and 1.2 g cm⁻³, respectively. When the soil was began to be packed, firstly, a 5-cm-thick sand layer with the total porosity of 49% and saturated hydraulic conductivity of 5.91 mm min⁻¹ was packed at the bottom of the soil pan. Then, the test soil was packed in the soil pan over the sand layer. The soil was packed to a depth of 20 cm. In order to compact the test soil to the same degree, the test soil was packed in four 5-cm layers. Firstly, the soil amount of each layer was kept as constant as possible to maintain a similar bulk density and uniform spatial distribution of soil particles. Secondly, the test soil of each packed soil layer was compacted to the designed bulk density before the next layer was packed to ensure uniformity in the soil structure.

2.4 Experiment procedures

After preparing the experiment soil pan, the rainfall intensity of 25 mm h⁻¹ was confirmed to pre-wet the soil pan. A nylon net cover was used to cover the soil pan in order to create uniform soil surface moisture conditions and reduce variability in soil surface micro-relief which developed

during the packing process. This design was consistent with that reported by An et al. (2012). Then, 1 day (i.e. 24 h) after the pre-rain phase, the simulated rainfall experiments were begun. In the process of the simulated rainfall experiment for each combination of slope gradient and rainfall intensity, rainfall lasted approximately 42 min in the stimulated rainfall experiment with no rill erosion. Samples of runoff produced by simulated rainfall were first collected for 1 min and 2 min after the onset of the runoff, and then for every 3 min until the end of the simulated rainfall experiment. Fifteen runoff samples were collected. In addition to sampling runoff, flow velocity was measured using KMnO₄ as a tracer, which was easy to identify in runoff. Surface flow velocity, which was measured from the middle of the test area, was measured 15 times for each treatment; then, a correction coefficient, which is 0.67 for laminar flow, 0.7 for transitional flow, and 0.8 for turbulent flow (Li and Abrahams 1999; An et al. 2012), was used to determine the flow velocity of laminar flow in this study. The interrill erosion samples (including runoff and sediments) were weighed and left to sit to allow suspended particles to settle. The clear supernatant was decanted, and the sediments left were oven-dried at 105 °C for 24 h to determine the sediment weight. The runoff weight was determined based on the difference value between interrill erosion samples weight and sediment weight. The runoff rate was defined as the runoff volume per unit area per unit time. The interrill erosion rate was defined as interrill erosion weight per unit area per unit time.

2.5 Data analysis

The data set was used to derive new equations which could describe the relationship of time to runoff, flow velocity, runoff rate and interrill erosion rate with slope gradient via regression analysis under different rainfall intensities. The statistical parameters R², MSE and NSE were used to evaluate the performance of new equations. The values of R², MSE and NSE were calculated as follows:

$$R^2 = \frac{\left[\sum_{i=1}^n (O_i - \bar{O})(P_i - \bar{P}) \right]^2}{\sum_{i=1}^n (O_i - \bar{O})^2 \sum_{i=1}^n (P_i - \bar{P})^2}, \quad (1)$$

$$MSE = \sqrt{\frac{\sum_{i=1}^n (O_i - P_i)^2}{n}}, \quad (2)$$

$$NSE = 1 - \frac{\sum (O_i - P_i)^2}{\sum (O_i - \bar{O})^2}, \quad (3)$$

where O_i are the observed values; P_i are the predicted values; \bar{O} is the mean of the observed value; \bar{P} is the mean of the predicted value; R^2 is the coefficient of determination; MSE is the residual mean; and NSE (Nash and Sutcliffe 1970) is a normalized statistic that reflects the relative magnitude of the residual variance compared with the variance of the observed data [good (NSE > 0.7)] (Moriiasi et al. 2007; Ahmad et al. 2011).

3 Results

3.1 The response of time to runoff to slope gradient

Figure 1 shows the response of time to runoff to slope gradient under three rainfall intensities from 90 to 150 mm h⁻¹. Evidently, the time to runoff was strongly influenced by the slope gradient under different rainfall intensities. The time to runoff decreased with increasing

slope gradients under different rainfall intensities. Furthermore, for the same rainfall intensity level, the time to runoff decreased with the slope gradient more rapidly when the rainfall intensity decreased from 150 to 90 mm h⁻¹, and this result indicated that the influence of slope gradient to time to runoff decreased gradually when the rainfall intensity increased from 90 to 150 mm h⁻¹.

In order to evaluate the relationship of time to runoff with slope gradient and quantify the influence of slope gradient to time to runoff, regression analyses were conducted to get the relationships which are shown in Table 1. Apparently, the time to runoff decreased as a linear function with increasing slope gradient. In Eqs. (4)–(6), the slope of the equations derived to evaluate and quantify the relationship between time to runoff and slope gradient under the rainfall intensity of 90, 120 and 150 mm h⁻¹ were -0.075, -0.03 and -0.014, respectively. The critical slope gradient under the rainfall intensity of 90, 120 and 150 mm h⁻¹ were

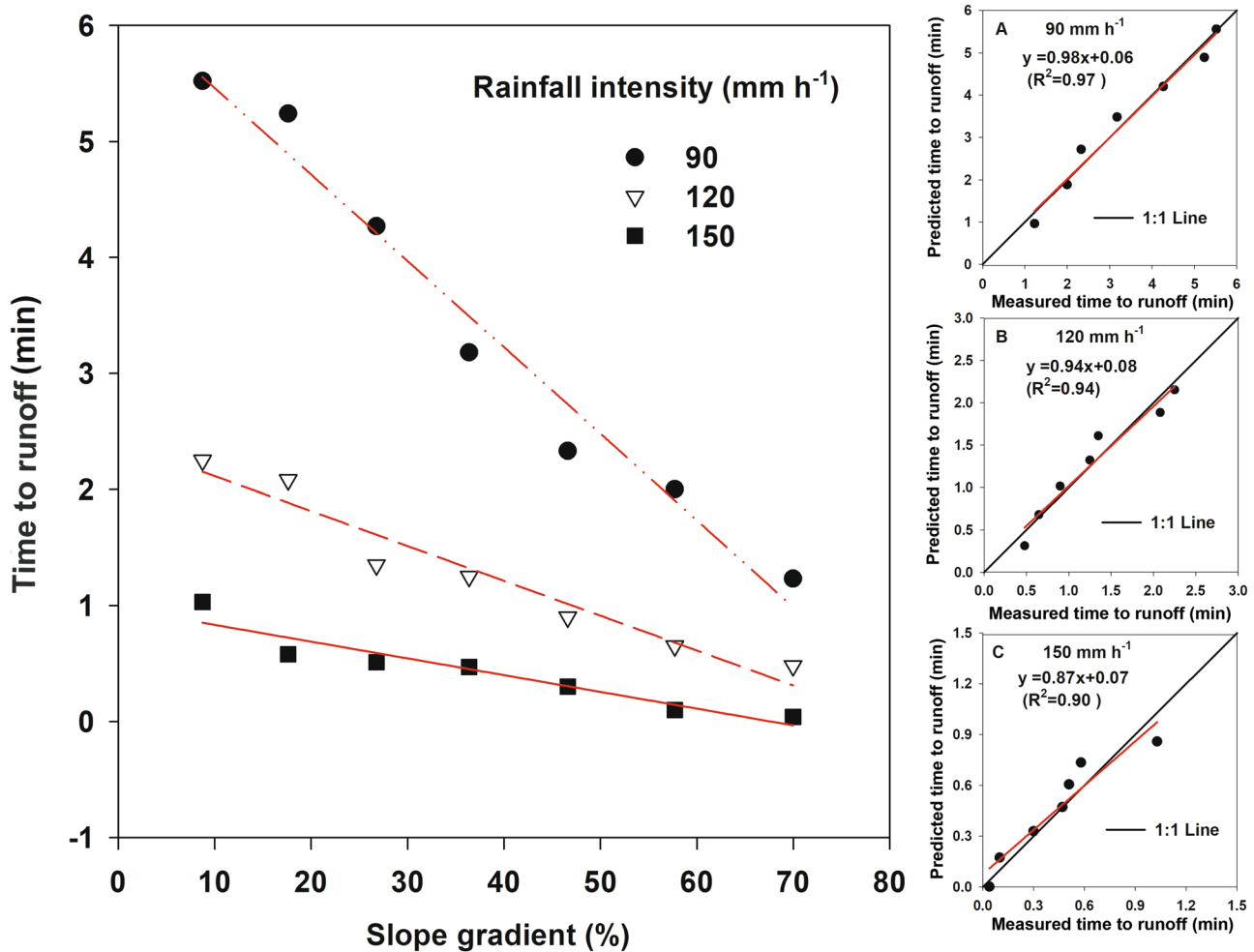


Fig. 1 The influence of slope gradient on time to runoff under three rainfall intensities

Table 1 Statistical equations of time to runoff (*RT*) varying with slope gradient (*S*) under different rainfall intensities and statistical evaluation of these new equations based on observed and predicted values

Rainfall intensity (mm h ⁻¹)	Equations (4)–(6)	<i>MSE</i>	<i>R</i> ²	<i>NSE</i>	<i>P</i>	<i>n</i>
90	$RT = -0.075(S - 82.8)$ (4)	0.25	0.97	0.97	0.01	7
120	$RT = -0.03(S - 80.33)$ (5)	0.15	0.94	0.94	0.01	7
150	$RT = -0.014(S - 70)$ (6)	0.1	0.90	0.90	0.01	7

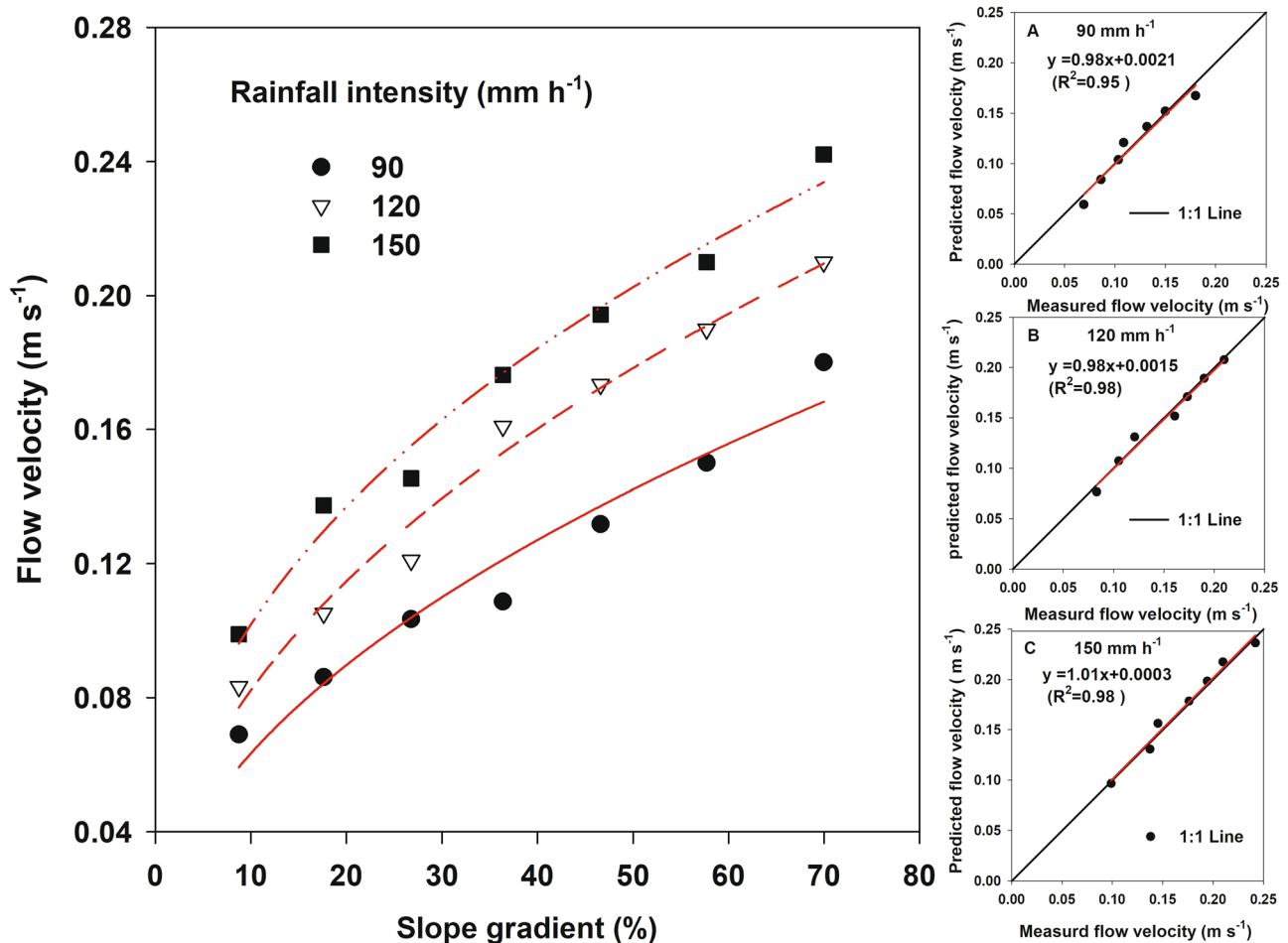
RT time to runoff (min), *S* slope gradient (%), *MSE* residual mean, *R*² coefficient of determination, *NSE* coefficient of Nash–Sutcliffe model efficiency

82.8%, 80.33% and 70%, respectively. *RT* is high with *R*² from 0.90 to 0.97 and significantly (*P* < 0.01) correlated with *S* under different rainfall intensities; *S* was a good predictor of *RT* for different rainfall intensities with *NSE* from 0.90 to 0.97. Figure 1 also presents the comparison between the predicted values of *RT* derived with Eqs. (4)–(6) and the measured values of *RT*. The 1:1 line of measured vs. predicted *RT* shows the high level of agreement between the predicted and observed values of *RT* with

NSE from 0.90 to 0.97 and *MSE* from 0.1 to 0.25 and *R*² from 0.90 to 0.97.

3.2 The response of flow velocity to slope gradient

Figure 2 shows the response of flow velocity to slope gradient under three rainfall intensities from 90 to 150 mm h⁻¹. Evidently, the flow velocity was strongly influenced by slope gradient under different rainfall intensities. The flow

**Fig. 2** The influence of slope gradient on flow velocity under three rainfall intensities

velocity increased obviously with increasing slope gradients under different rainfall intensities.

In order to evaluate the relationship of flow velocity with slope gradient and quantify the influence of slope gradient to flow velocity, regression analyses were conducted to get the relationships which are shown in Table 2. Apparently, the flow velocity increased as a power function with increasing slope gradients; the coefficients of the equations under 90, 120 and 150 mm h⁻¹ rainfall intensities were 0.02, 0.027 and 0.038, respectively; and the exponents of slope gradient under 90, 120 and 150 mm h⁻¹ rainfall intensities were 0.50, 0.48 and 0.43, respectively. *V* is high with *R*² from 0.95 to 0.98 and significantly (*P* < 0.01) correlated with *S* under different rainfall intensities; *S* was a good predictor of *V* for different rainfall intensities with *NSE* from 0.91 to 0.93. Figure 2 also presents the comparison between the predicted values of *V* derived with Eqs. (7)–(9) and the measured values of *V*. The 1:1 line of measured vs. predicted *V* shows the high level of agreement between the predicted and observed values of *V* with *NSE* from 0.91 to 0.93 and *MSE* from 0.01 to 0.015 and *R*² from 0.95 to 0.98.

3.3 The response of runoff rate to slope gradient

Figure 3 shows the response of runoff rate to slope gradient under three rainfall intensities from 90 to 150 mm h⁻¹. Evidently, the runoff rate was influenced by slope gradient under different rainfall intensities. The runoff rate increased with increasing slope gradients under different rainfall intensities.

In order to evaluate the relationship of the runoff rate with slope gradient and quantify the influence of slope gradient to runoff rate, regression analyses were conducted to get the relationships which are shown in Table 3. Apparently, the runoff rate increased as a power function with increasing slope gradients; the coefficients of the equations under 90, 120 and 150 mm h⁻¹ rainfall intensities were 0.00000013, 0.00000092 and 0.00000126, respectively; and the exponents of slope gradient under 90, 120 and 150 mm h⁻¹ rainfall intensities were 0.47, 0.1 and 0.08, respectively. *RR* is high with *R*² from 0.94 to 0.97

and significantly (*P* < 0.01) correlated with *S* under different rainfall intensities; *S* was a good predictor of *RR* for different rainfall intensities with *NSE* from 0.90 to 0.95. Figure 2 also presents the comparison between the predicted values of *RR* derived with Eqs. (10)–(12) and the measured values of *RR*. The 1:1 line of measured vs. predicted *RR* shows the high level of agreement between the predicted and observed values of *RR* with *NSE* from 0.90 to 0.95 and *MSE* from 0.000000024 to 0.000000044 and *R*² from 0.94 to 0.97.

3.4 The response of interrill erosion rate to slope gradient

Figure 4 shows the response of interrill erosion rate to slope gradient under three rainfall intensities from 90 to 150 mm h⁻¹. Evidently, the interrill erosion rate was strongly influenced by slope gradient under different rainfall intensities. The interrill erosion rate increased obviously with increasing slope gradients under different rainfall intensities.

In order to evaluate the relationship of interrill erosion rate with slope gradient and quantify the influence of slope gradient to interrill erosion rate, regression analyses were conducted to get the relationships which are shown in Table 4. Apparently, the interrill erosion rate increased as a power function with increasing slope gradients; the coefficients of the equations under 90, 120 and 150 rainfall intensities were 0.0000000392, 0.000000721 and 0.00000352, respectively, and the exponents of slope gradient under 90, 120 and 150 rainfall intensities were 2.9, 2.3 and 1.97, respectively. *IER* is high with *R*² from 0.98 to 0.99 and significantly (*P* < 0.01) correlated with *S* under different rainfall intensities; *S* was a good predictor of *IER* for different rainfall intensities with *NSE* from 0.98 to 0.99. Figure 2 also presents the comparison between the predicted values of *V* derived with Eqs. (13)–(15) and the measured values of *IER*. The 1:1 line of measured vs. predicted *IER* shows the high level of agreement between the predicted and observed values of *IER* with *NSE* from 0.98 to 0.99 and *MSE* from 0.0002 to 0.00055 and *R*² from 0.98 to 0.99.

Table 2 Statistical equations of flow velocity (*V*) varying with slope gradient (*S*) under different rainfall intensities and statistical evaluation of these new equations based on observed and predicted values

Rainfall intensity (mm h ⁻¹)	Equations (7)–(9)	<i>MSE</i>	<i>R</i> ²	<i>NSE</i>	<i>P</i>	<i>n</i>
90	$V = 0.02S^{0.5}$ (7)	0.01	0.95	0.91	0.01	7
120	$V = 0.027S^{0.48}$ (8)	0.015	0.98	0.91	0.01	7
150	$V = 0.038S^{0.43}$ (9)	0.013	0.98	0.93	0.01	7

V flow velocity (m s⁻¹), *S* slope gradient (%), *MSE* residual mean, *R*² coefficient of determination, *NSE* coefficient of Nash–Sutcliffe model efficiency

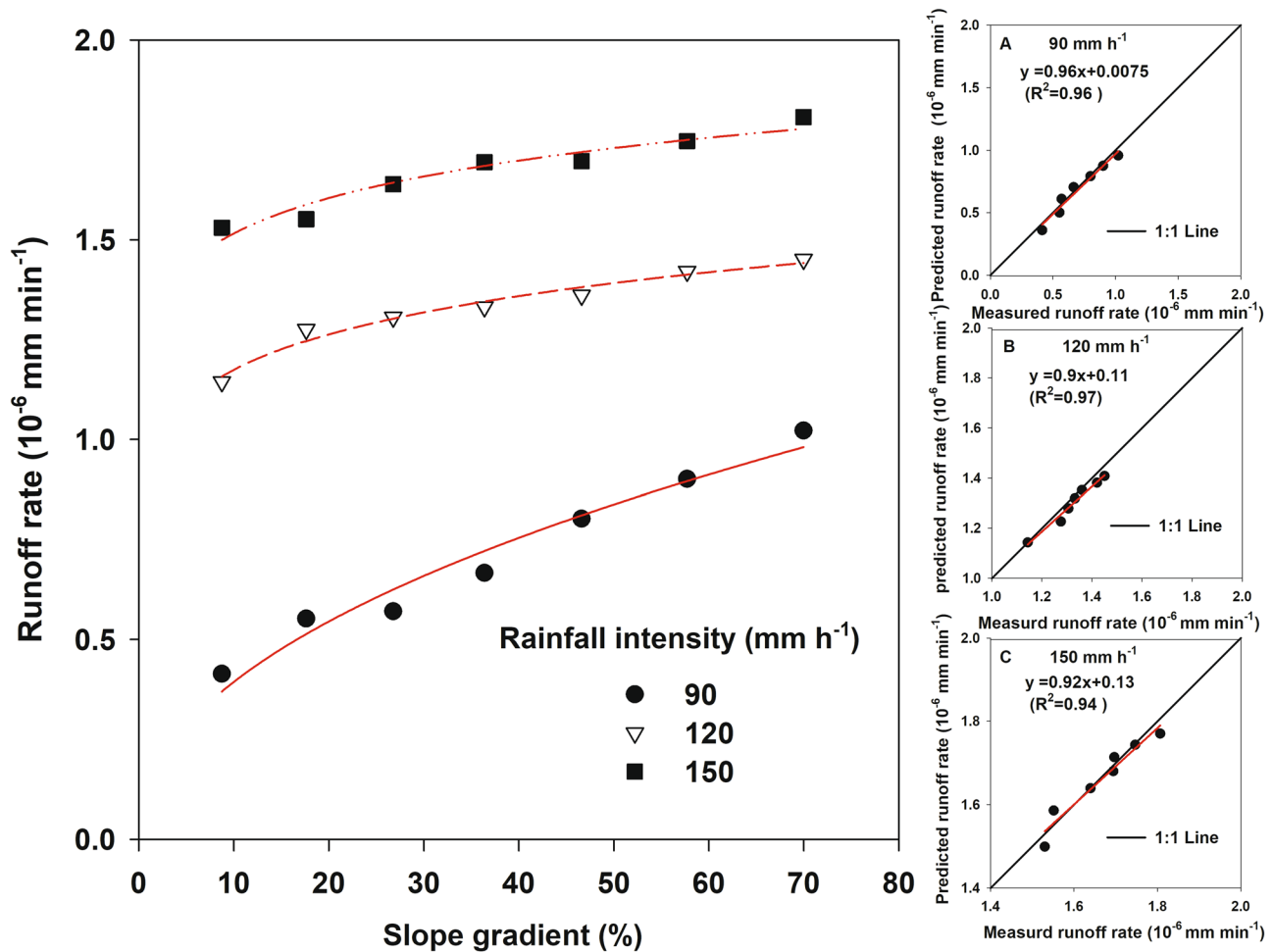


Fig. 3 The influence of slope gradient on runoff rate under three rainfall intensities

4 Discussion

In this study, the time to runoff decreased as a linear function with increasing slope gradient. Many studies indicated that vegetation cover and antecedent soil moisture are considered as main factors that can affect time to runoff and the time to runoff increased as vegetation cover increases (Guanghui and Yimin 1995; Li et al. 2005; Yang et al. 2014), which decreased as antecedent soil moisture increases (Lado et al. 2004; Liu et al. 2011); however, few studies have shown the effect of slope on the time to runoff under the condition

of same antecedent soil moisture and no vegetation cover. This result indicated that slope gradient have an important effect on time to runoff when the slope gradients were from 8.74 to 69.97%. The flow velocity increased as slope gradients increase. This result was consistent with the finding of Zhuang et al. (2018) and Wu et al. (2017b). The relationship of slope gradient and flow velocity can be described by a power function. This result was consistent with the finding of Wu et al. (2017b). In fact, the relationship between runoff velocity and slope gradient is probably due to gravitational force (Zhuang et al. 2018), surface roughness (Govers 1992;

Table 3 Statistical equations of runoff rate (RR) varying with slope gradient (S) under different rainfall intensities and statistical evaluation of these new equations based on observed and predicted values

Rainfall intensity (mm h ⁻¹)	Equations (10)–(12)	MSE	R ²	NSE	P	n
90	$RR = (0.13 \times 10^{-6})S^{0.47}$ (10)	4.4×10^{-8}	0.96	0.95	0.01	7
120	$RR = (0.92 \times 10^{-6})S^{0.1}$ (11)	3.22×10^{-8}	0.97	0.90	0.01	7
150	$RR = (1.26 \times 10^{-6})S^{0.08}$ (12)	2.39×10^{-8}	0.94	0.93	0.01	7

RR runoff rate (mm min⁻¹), S slope gradient (%), MSE residual mean, R² coefficient of determination, NSE coefficient of Nash–Sutcliffe model efficiency

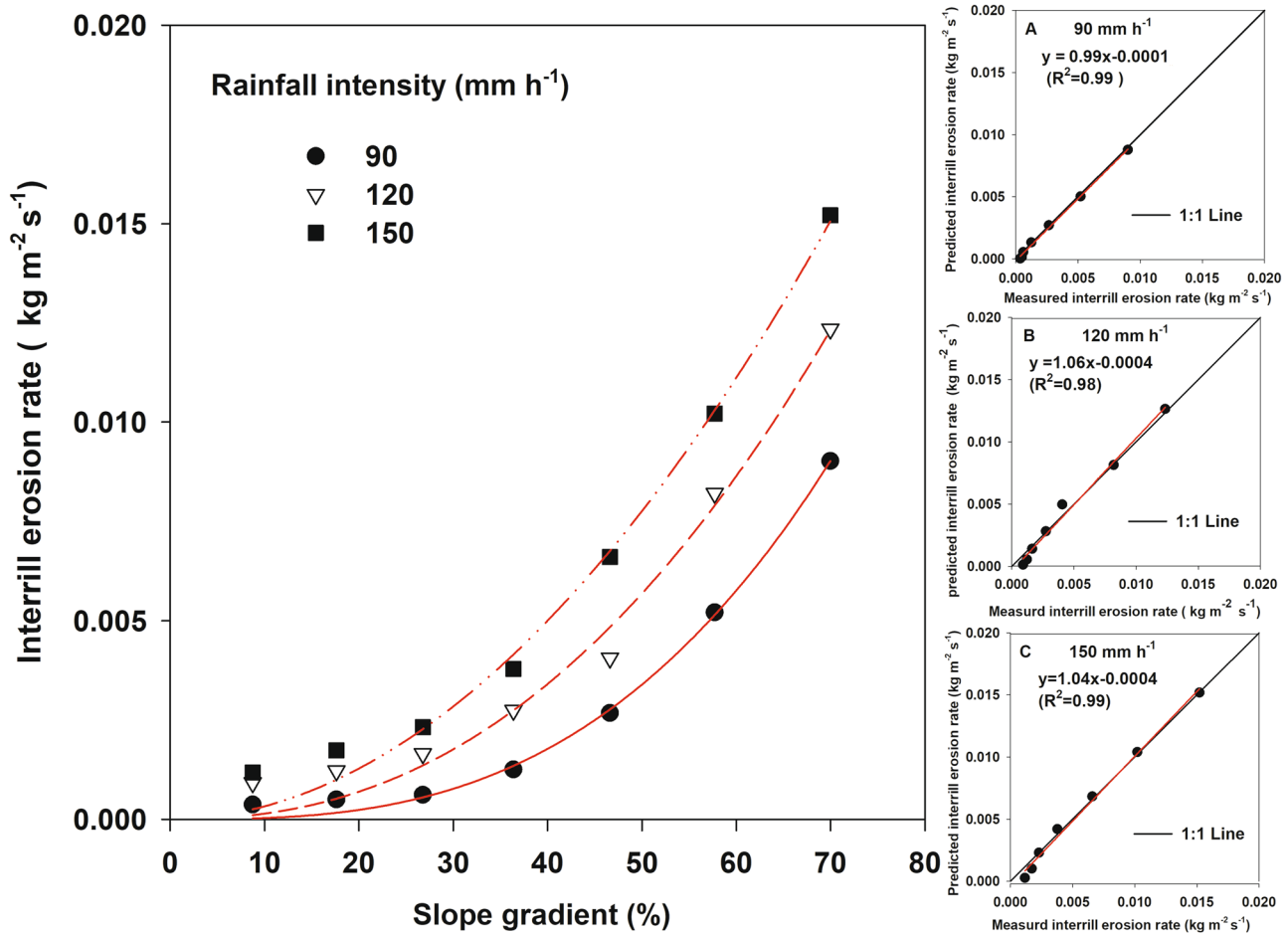


Fig. 4 The influence of slope gradient on interrill erosion rate under three rainfall intensities

Nearing et al. 1997, 1999; Takken et al. 1998; Fox and Bryan 2000; Giménez and Govers 2001; Ali et al. 2011), sediment load (Zhang et al. 2010), and soil particles (Wu et al. 2016) under the same rainfall intensity. In our study, the runoff rate increased as a power function with increasing slope gradients. Firstly, a major influence of slope gradient on runoff rate appears to be exerted through its impact on runoff velocity. Secondly, the explanation for this was that the infiltration rate decreased with increasing slope gradient. Most studies on runoff rate focused on the change of runoff rate over time under different slope gradients, different rainfall intensities and different slope surface conditions, and the

effect of slope on runoff rate is neglected. The interrill erosion rate also increased as a power function with increasing slope gradients. This result was consistent with the finding by Assouline and Ben-Hur (2006) and Wu et al. (2017a, b, c). By contrast, Huang and Bradford (1993) found that the linear functions that existed between interrill erosion rate and slope gradient for three rainfall intensities and slope gradients were 5%, 9% and 20%. The variation in result was likely attributed to slope gradient and soil surface conditions. Firstly, seven slope gradients ranging from 8.74 to 69.97% were selected in our study, and thus, the result of the regression analysis could be more accurate. It is important

Table 4 Statistical equations of interrill erosion rate (*IER*) varying with slope gradient (*S*) under different rainfall intensities and statistical evaluation of these new equations based on observed and predicted values

Rainfall intensity (mm h ⁻¹)	Equations (13)–(15)	<i>MSE</i>	<i>R</i> ²	<i>NSE</i>	<i>P</i>	<i>n</i>
90	$IER = (3.92 \times 10^{-8})S^{2.9}$ (13)	0.0002	0.99	0.99	0.01	7
120	$IER = (7.21 \times 10^{-7})S^{2.3}$ (14)	0.00055	0.98	0.98	0.01	7
150	$IER = (3.52 \times 10^{-6})S^{1.97}$ (15)	0.00048	0.99	0.99	0.01	7

IER interrill erosion rate (kg m⁻² s⁻¹), *S* slope gradient (%), *MSE* residual mean, *R*² coefficient of determination, *NSE* coefficient of Nash–Sutcliffe model efficiency

to show that the interrill erosion rate was very sensitive to changes in slope gradient. Then, soil surface conditions such as soil moisture, roughness and slope length significantly affect interrill erosion.

5 Conclusion

In this study, the response of interrill erosion processes (i.e. time to runoff, flow velocity, runoff rate, interrill erosion rate) to slope gradient was investigated using simulated rainfall. The results of this study demonstrated that slope gradients have an important influence on interrill erosion processes. The time to runoff decreased as a linear function with increasing slope gradients under different rainfall intensities, but the flow velocity, runoff rate and interrill erosion rate were increased obviously as a power function with increasing slope gradients under different rainfall intensities.

Slope gradient was a good predictor of time to runoff for different rainfall intensities with NSE from 0.90 to 0.97 and MSE from 0.1 to 0.25 and R^2 from 0.90 to 0.97. Slope gradient could be used to predict flow velocity for different rainfall intensities with NSE from 0.91 to 0.93 and MSE from 0.01 to 0.015 and R^2 from 0.95 to 0.98. Slope gradient was also a good predictor of runoff rate for different rainfall intensities with NSE from 0.90 to 0.95 and MSE from 2.4×10^{-8} to 4.4×10^{-8} and R^2 from 0.94 to 0.97. Slope gradient could be used satisfactorily to predict interrill erosion rate for different rainfall intensities with NSE from 0.98 to 0.99 and MSE from 0.00022 to 0.00055 and R^2 from 0.98 to 0.99. These findings can facilitate the evaluation of the influence of slope gradient to interrill erosion processes under our study conditions; additional research is needed to develop equations/models that can be universally applied to evaluate the influence of slope gradient to interrill erosion processes.

Funding Financial support for this research was provided by the National Natural Science Foundation of China–funded project (41907046, 41790441, 41772316, 41830758); project funded by the China Postdoctoral Science Foundation (2018M640998); project supported by the State Key Laboratory of Earth Surface Processes and Resource Ecology (2020-KF-08); project supported by the State Key Laboratory of Soil Erosion and Dryland Farming on the Loess Plateau (A314021402-2001); and the National Key Research and Development Program of China (2018YFC1504701).

References

- Ahmad N, Hafiz M, Sinclair A, Jamieson R, Madani A, Hebb D, Yiridoe EK (2011) Modeling sediment and nitrogen export from a rural watershed in Eastern Canada using the soil and water assessment tool. *J Environ Quality* 40:1182–1194
- An J, Zheng F, Lu J, Li G (2012) Investigating the role of raindrop impact on hydrodynamic mechanism of soil erosion under simulated rainfall conditions. *Soil Sci* 177:517–526
- Armstrong A, Quinton JN, Heng BCP, Chandler JH (2011) Variability of interrill erosion at low slopes. *Earth Surf Process Land* 36:97–106
- Ali M, Sterk G, Seeger M, Boersema MP, Peters P (2011) Effect of hydraulic parameters on sediment transport capacity in overland flow over erodible beds. *Hydrol Earth Syst Sci Discuss* 8:6939–6965
- Assouline S, Ben-Hur M (2006) Effects of rainfall intensity and slope gradient on the dynamics of interrill erosion during soil surface sealing. *Catena* 66:211–220
- Ben-Hur M, Wakindiki IIC (2004) Soil mineralogy and slope effects on infiltration, interrill erosion, and slope factor. *Water Resour Res* 40:1–8
- Cao L, Zhang K, Dai H, Liang Y (2015) Modeling interrill erosion on unpaved roads in the loess plateau of China. *Land Degrad Dev* 26:825–832
- Ding W, Huang C (2017) Effects of soil surface roughness on interrill erosion processes and sediment particle size distribution. *Geomorphology* 295:801–810
- Fox DM, Bryan RB (2000) The relationship of soil loss by interrill erosion to slope gradient. *Catena* 38:211–222
- Fu S, Liu B, Liu H, Xu L (2011) The effect of slope on interrill erosion at short slopes. *Catena* 84:29–34
- Giménez R, Govers G (2001) Interaction between bed roughness and flow hydraulics in eroding rills. *Water Resour Res* 37:791–799
- Govers G (1992) Relationship between discharge, velocity and flow area for rills eroding loose, non-layered materials. *Earth Surf Proc Land* 17:515–528
- Guanghui Z, Yimin L (1995) Study on runoff beginning time of artificial grassland in loess hilly region. *J Soil Water Conserv* 9:78–83
- Huang CH, Bradford JM (1993) Analyses of slope and runoff factors based on the WEPP erosion model. *Soil Sci Soc Am J* 57:1176–1183
- Lado M, Ben-Hur M, Shainberg I (2004) Soil wetting and texture effects on aggregate stability, seal formation, and erosion. *Soil Sci Soc Am J* 68:1992–1999
- Li C, Holden J, Grayson R (2018) Effects of rainfall, overland flow and their interactions on peatland interrill erosion processes. *Earth Surf Proc Land* 43:1451–1464
- Li G, Abrahams AD (1999) Controls of sediment transport capacity in laminar interrill flow on stone-covered surfaces. *Water Resour Res* 5(1):305–310
- Li M, Yao W, Li Z (2005) Progress of the effect of grassland vegetation for conserving soil and water on loess plateau. *Adv Earth Sci* 20:74–080
- Liu G, Xu WN, Zhang Q, Xia ZY (2012a) Interrill and rill erosion on hillslope. *Appl Mech Mater* 170–173:1344–1347
- Liu H, Lei TW, Zhao J, Yuan CP, Fan YT, Qu LQ (2011) Effects of rainfall intensity and antecedent soil water content on soil infiltrability under rainfall conditions using the run off-on-out method. *J Hydrol* 396:24–32
- Liu Y, Fu B, Lü Y, Wang Z, Gao G (2012b) Hydrological responses and soil erosion potential of abandoned cropland in the Loess Plateau, China. *Geomorphology* 138:404–414
- Moriasi DN, Arnold JG, Van Liew MW, Bingner RL, Harmel RD, Veith TL (2007) Model evaluation guidelines for systematic quantification of accuracy in watershed simulations. *T ASABE* 50:885–900
- Nash JE, Sutcliffe JV (1970) River flow forecasting through conceptual models part I—a discussion of principles. *J Hydrol* 10:282–290

- Nearing MA, Norton LD, Bulgakov DA, Larionov GA, West LT, Dontsova KM (1997) Hydraulics and erosion in eroding rills. *Water Resour Res* 33:865–876
- Nearing MA, Simanton JR, Norton LD, Bulygin SJ, Stone J (1999) Soil erosion by surface water flow on a stony, semiarid hillslope. *Earth Surf Process Landf: J Br Geomorph Res Group* 24:677–686
- Shen H, Zheng F, Wen L, Han Y, Hu W (2016) Impacts of rainfall intensity and slope gradient on rill erosion processes at loessial hillslope. *Soil Tillage Res* 155:429–436
- Shi H, Shao M (2000) Soil and water loss from the Loess Plateau in China. *J Arid Environ* 45:9–20
- Shi ZH, Yue BJ, Wang L, Fang NF, Wang D, Wu FZ (2013) Effects of mulch cover rate on interrill erosion processes and the size selectivity of eroded sediment on steep slopes. *Soil Sci Soc Am J* 77:257–267
- Takken I, Govers G, Ciesiolka CAA, Silburn DM, Loch RJ (1998) Factors influencing the velocity–discharge relationship in rills. *IAHS Publication*, p 63–70
- Vaezi AR, Ahmadi M, Cerdà A (2017) Contribution of raindrop impact to the change of soil physical properties and water erosion under semi-arid rainfalls. *Sci Total Environ* 583:382–392
- Wang D, Wang Z, Zhang Q, Zhang Q, Tian N, Liu JE (2018) Sheet erosion rates and erosion control on steep rangelands in loess regions. *Earth Surf Proc Land* 43:2926–2934
- Wu B, Wang Z, Shen N, Wang S (2016) Modelling sediment transport capacity of rill flow for loess sediments on steep slopes. *Catena* 147:453–462
- Wu B, Wang Z, Zhang Q, Shen N (2018) Distinguishing transport-limited and detachment-limited processes of interrill erosion on steep slopes in the Chinese loessial region. *Soil Tillage Res* 177:88–96
- Wu B, Wang Z, Zhang Q (2017a) Modelling sheet erosion on steep slopes in the loess region of china. *J Hydrol* 553:549–558
- Wu L, Wang S, Bai X, Luo W, Tian Y, Zeng C, He S (2017b) Quantitative assessment of the impacts of climate change and human activities on runoff change in a typical karst watershed, SW China. *Sci Total Environ* 601:1449–1465
- Wu S, Yu M, Chen L (2017c) Nonmonotonic and spatial-temporal dynamic slope effects on soil erosion during rainfall-runoff processes. *Water Resour Res* 53:1369–1389
- Yang Y, Ye Z, Liu B, Zeng X, Fu S, Lu B (2014) Nitrogen enrichment in runoff sediments as affected by soil texture in Beijing mountain area. *Environ Monit Assess* 186:971–978
- Zhang Q, Wang Z, Guo Q, Tian N, Shen N, Liu JE (2019) Plot-based experimental study of raindrop detachment, interrill wash and erosion-limiting degree on a clayey loessial soil. *J Hydrol* 575:1280–1287
- Zhang Q, Xu CY, Zhang Z, Chen X, Han Z (2010) Precipitation extremes in a karst region: a case study in the Guizhou province, southwest China. *Theor Appl Climatol* 101:53–65
- Zhang XC, Liu WZ, Li Z, Zheng FL (2009) Simulating site-specific impacts of climate change on soil erosion and surface hydrology in southern Loess Plateau of China. *Catena* 79:237–242
- Zhang XJ, Wang ZL (2017) Interrill soil erosion processes on steep slopes. *J Hydrol* 548:652–664
- Zhang XC (2019) Determining and modeling dominant processes of interrill soil erosion. *Water Resour Res* 55:4–20
- Zhao G, Mu X, Wen Z, Wang F, Gao P (2013) Soil erosion, conservation, and eco-environment changes in the Loess Plateau of China. *Land Degrad Dev* 24:499–510
- Zhao L, Liang X, Wu F (2014) Soil surface roughness change and its effect on runoff and erosion on the Loess Plateau of China. *J Arid Land* 6:400–409
- Zhuang X, Wang W, Ma Y, Huang X, Lei T (2018) Spatial distribution of sheet flow velocity along slope under simulated rainfall conditions. *Geoderma* 321:1–7

Publisher's Note Springer Nature remains neutral with regard to jurisdictional claims in published maps and institutional affiliations.